Geochemistry Geophysics Geosystems G3
AN ELECTRONIC JOURNAL OF THE EARTH SCIENCES
Published by AGU and the Geochemical Society

Article
Volume 7, Number 12
15 December 2006
Q12003, doi:10.1029/2006GC001323
ISSN: 1525-2027

Deep water mass geometry in the glacial Atlantic Ocean: A review of constraints from the paleonutrient proxy Cd/Ca

Thomas M. Marchitto
Department of Geological Sciences and Institute of Arctic and Alpine Research, University of Colorado, Boulder, Colorado, 80309, USA (tom.marchitto@colorado.edu)

Wallace S. Broecker
Lamont-Doherty Earth Observatory of Columbia University, Palisades, New York, 10964, USA (broecker@ldeo.columbia.edu)

[1] Paleonutrient proxies currently provide the strongest constraints on the past spatial distribution of deep water masses. We review the state of knowledge derived from the trace metal proxy Cd/Ca for the Atlantic Ocean during the Last Glacial Maximum (LGM). We compile published benthic foraminiferal Cd/Ca data, supplemented with new data, to reconstruct meridional Cd sections through the Holocene and LGM Atlantic. Holocene Cd/Ca reflects the modern water masses North Atlantic Deep Water (NADW), Antarctic Bottom Water (AABW), and Antarctic Intermediate Water (AAIW) reasonably well, except for anomalously high values in the intermediate to mid-depth far North Atlantic. LGM Cd/Ca clearly shows that NADW was replaced by the shallower Glacial North Atlantic Intermediate Water (GNAIW), with significant northward expansion of AABW. The boundary level between GNAIW and AABW was very abrupt, occurring between ~2200 and 2500 m modern water depth. Combined Cd/Ca and *Cibicidoides* $\delta^{13}C$ data allow us to also calculate the air-sea signature of $\delta^{13}C$ ($\delta^{13}C_{as}$). The LGM Atlantic can be explained entirely by mixing between high-$\delta^{13}C_{as}$ GNAIW and low-$\delta^{13}C_{as}$ AABW. Negative $\delta^{13}C_{as}$ values in glacial AABW were likely caused by poor ventilation during formation, probably associated with extensive sea ice coverage. Overall, our knowledge base would benefit from improved data coverage in the South Atlantic and Southern Ocean, and a better understanding of ancillary effects on the Cd/Ca proxy itself.

Components: 9658 words, 6 figures, 3 tables.

Keywords: cadmium; $\delta^{13}C$; air-sea.

Index Terms: 4924 Paleoceanography: Geochemical tracers; 4926 Paleoceanography: Glacial; 4962 Paleoceanography: Thermohaline.

Received 1 April 2006; **Revised** 1 September 2006; **Accepted** 28 September 2006; **Published** 15 December 2006.

Marchitto, T. M., and W. S. Broecker (2006), Deep water mass geometry in the glacial Atlantic Ocean: A review of constraints from the paleonutrient proxy Cd/Ca, *Geochem. Geophys. Geosyst.*, *7*, Q12003, doi:10.1029/2006GC001323.

1. Introduction

[2] Past changes in the ocean's Meridional Overturning Circulation (MOC) are believed to have significantly impacted regional climates by altering patterns of ocean heat transport. In particular, changes in the strength and/or location of North Atlantic Deep Water (NADW) formation likely

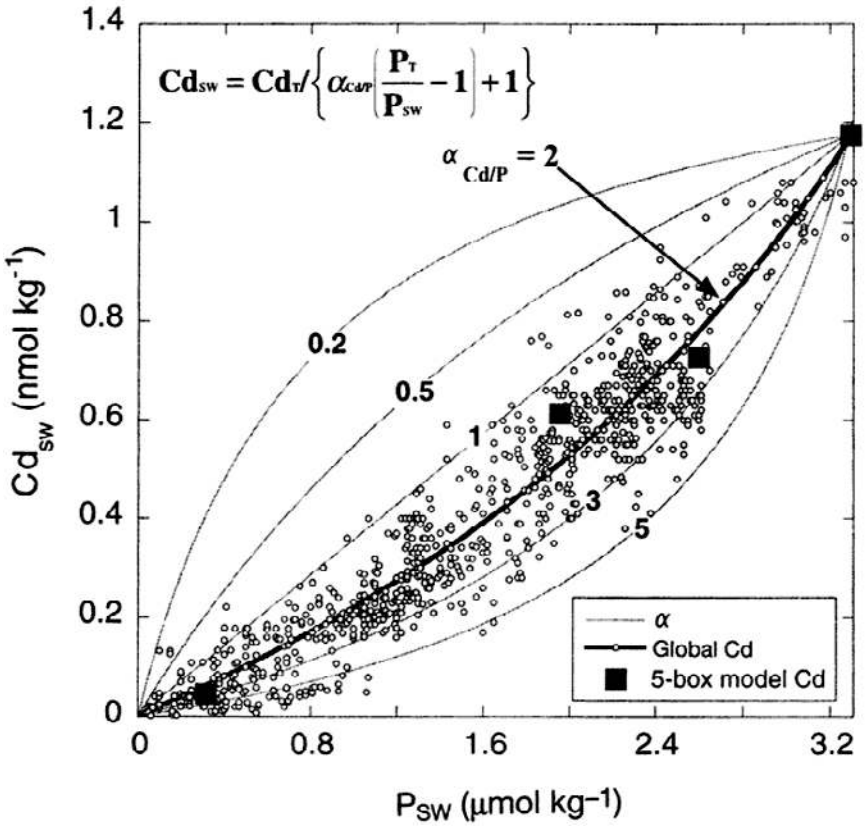

Figure 1. Dissolved Cd versus dissolved phosphate in the global ocean, reproduced from *Elderfield and Rickaby* [2000]. Curves show different solutions to the inset equation (equation (1) with $Cd_T = 1.2$ and $P_T = 3.3$) that can explain regional relationships between the two nutrients. Bold line is the best fit to the global data set, with $\alpha_{Cd/P} = 2$. Reprinted by permission from Macmillan Publishers Ltd.

caused the abrupt millennial-scale warmings and coolings that characterized the climate of the North Atlantic region during the last glaciation [e.g., *Broecker et al.*, 1985; *Stocker and Wright*, 1991; *Ganopolski and Rahmstorf*, 2001; *Rahmstorf*, 2002]. The climatic footprint of these so-called Dansgaard-Oeschger events was large, including notable impacts on the position of the Atlantic Intertropical Convergence Zone (ITCZ) [*Peterson et al.*, 2000], the strength of the Asian monsoons [*Schulz et al.*, 1998; *Wang et al.*, 2001], and the intensity of the northeastern tropical Pacific oxygen minimum zone [*Behl and Kennett*, 1996; *Ortiz et al.*, 2004]. In addition, glacial modes of deep ocean circulation may have fundamentally altered large-scale patterns of nutrient upwelling, biological production, and $CaCO_3$ preservation, thereby contributing to the drawdown of atmospheric CO_2 [e.g., *Broecker and Peng*, 1987; *Toggweiler*, 1999; *Sigman and Boyle*, 2000; *Marchitto et al.*, 2005; *Toggweiler et al.*, 2006].

[3] Most of what paleoceanographers know about the past distribution of deep water masses is derived from paleonutrient proxies. Such passive tracers offer no direct information about deep water formation rates or fluxes [*LeGrand and Wunsch*, 1995], but may be used to constrain conceptual and numerical models of the MOC. The most widely applied paleonutrient tracer is benthic foraminiferal $\delta^{13}C$, which is inversely correlated with the labile nutrient phosphate [*Kroopnick*, 1985; *Duplessy et al.*, 1988; *Sarnthein et al.*, 1994; *Curry and Oppo*, 2005]. Boyle and colleagues developed benthic foraminiferal Cd/Ca as a deep water tracer at about the same time that $\delta^{13}C$ was first applied to the problem, in the early 1980s [*Boyle and Keigwin*, 1982, 1985/1986]. Cd/Ca was therefore instrumental in codifying the view of a glacial-age shoaling of low-nutrient NADW and northward expansion of nutrient-rich Antarctic Bottom Water (AABW) into the North Atlantic [*Boyle and Keigwin*, 1987; *Oppo and Fairbanks*, 1987] (note that we use AABW to include Circumpolar Deep Water

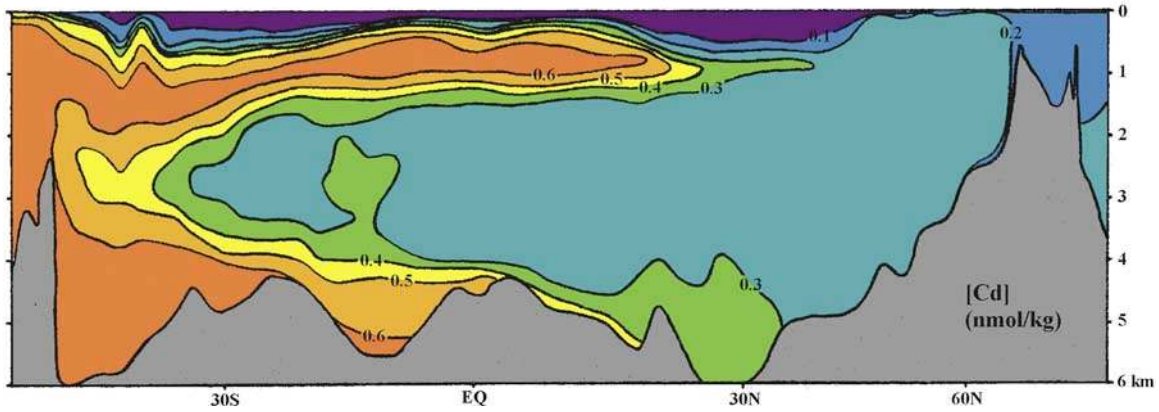

Figure 2. Inferred dissolved Cd concentrations in the modern western Atlantic Ocean, estimated from GEOSECS dissolved phosphate measurements [*Bainbridge*, 1981] and the Cd:phosphate global relationship of *Boyle* [1988]. Low-Cd NADW lies between high-Cd AABW below and AAIW above. After *Marchitto et al.* [2002].

(CPDW); the glacial version of AABW/CPDW has also sometimes been referred to as Southern Ocean Water). Benthic foraminiferal Ba/Ca [*Lea and Boyle*, 1989, 1990; *Martin and Lea*, 1998] and Zn/Ca [*Marchitto et al.*, 2000, 2002] have since been developed as complementary paleonutrient tracers, though their application has been very limited in comparison to Cd/Ca.

2. Cd/Ca Systematics

[4] Numerous dissolved trace elements in the ocean exhibit vertical profiles that resemble those of major nutrients [*Nozaki*, 1997]. That is, they are at low concentrations in surface waters and greater concentrations at depth. In some cases, this behavior is linked to the element's importance as a micronutrient. In other cases, nutrient-like behavior may simply result from adsorption onto particulate organic matter in the photic zone and co-remineralization in the deep sea. Regardless of biogeochemical mechanisms, such elements may be useful as nutrient and water mass tracers. Paleoceanographic applications rely on the observation that various elements are accidentally incorporated into benthic foraminiferal $CaCO_3$ during precipitation. In particular, divalent cations are believed to substitute for Ca in the $CaCO_3$ crystal matrix.

[5] Dissolved Cd has an oceanic distribution very similar to that of the nutrient phosphate [*Boyle et al.*, 1976; *Boyle*, 1988; *Elderfield and Rickaby*, 2000] (Figures 1 and 2). Both are efficiently removed from most surface waters and regenerated at depth, with an intermediate-depth concentration maximum near 1000 m. Cd therefore behaves like a labile nutrient, and its concentration increases about five-fold between the deep North Atlantic and North Pacific. Although Cd has been linked to at least one important algal metalloenzyme, carbonic anhydrase [*Cullen et al.*, 1999; *Morel et al.*, 2003], it is not clear if this use is sufficient to explain its ocean-wide nutrient-like behavior. The global correlation between Cd and phosphate follows a slight curve that may be explained by preferential uptake of Cd relative to phosphate, either actively by phytoplankton or passively by adsorption onto particulate organic matter [*Elderfield and Rickaby*, 2000] (Figure 1):

$$\mathrm{Cd} = 1.2/\left(\alpha_{\mathrm{Cd/P}}(3.3/\mathrm{P} - 1) + 1\right) \quad (1)$$

where $\alpha_{\mathrm{Cd/P}}$ is the ratio of Cd/P in particulate organic matter relative to Cd/P in seawater, and averages $\sim$2 for the global data set. Historically, however, the Cd:phosphate relationship has been described simply by two line segments [*Boyle*, 1988]:

$$\mathrm{Cd} = 0.208\mathrm{P}\ \left(\text{for P} < 1.34\ \mu\text{mol kg}^{-1}\right) \quad (2)$$

$$\mathrm{Cd} = 0.398\mathrm{P} - 0.254\left(\text{for P} > 1.34\ \mu\text{mol kg}^{-1}\right) \quad (3)$$

[6] Benthic foraminiferal Cd/Ca ratios reflect seawater dissolved Cd concentrations, with partition coefficients:

$$D_{\mathrm{Cd}} = (\mathrm{Cd/Ca})_{\mathrm{foram}}/(\mathrm{Cd/Ca})_{\mathrm{seawater}} \quad (4)$$

that vary with water depth in calcitic species, from a minimum of 1.3 above 1150 m to a maximum of 2.9 below 3000 m [*Boyle*, 1992]. The aragonitic benthic foraminifer *Hoeglundina elegans* has a partition coefficient of 1.0, apparently invariant with water depth [*Boyle et al.*, 1995]. Cd incorporation into benthic foraminifera does not

appear to be significantly affected by water temperature [*Marchitto*, 2004].

3. Challenges and Uncertainties

[7] Several ancillary effects may complicate the reconstruction of past Cd concentrations in seawater. First, many published records rely on combinations of benthic foraminiferal taxa, including epifaunal genera like *Cibicidoides* and infaunal genera like *Uvigerina*. Microhabitat is known to affect the $\delta^{13}C$ of infaunal taxa because of organic matter degradation within sediment pore waters [*Zahn et al.*, 1986; *McCorkle et al.*, 1997]. Yet *Boyle* [1992] has shown that there is no consistent Cd/Ca offset between the various calcitic taxa, regardless of microhabitat. *Tachikawa and Elderfield* [2002] suggest that infaunal species usually record Cd/Ca values similar to *Cibicidoides*, despite elevated pore water Cd, because they have lower partition coefficients. If true, it would seem to be fortuitous that *Cibicidoides* and *Uvigerina* have successfully been used interchangeably in paleoceanographic reconstructions. Our own compilation of published data (section 5.1) indicates that there is no significant bias if infaunal species are included. Nevertheless, improved understanding of possible species-level differences and microhabitat effects is essential.

[8] Benthic foraminiferal trace metal partition coefficients are further affected by seawater saturation state with respect to calcite (ΔCO_3^{2-}). D_{Cd}, D_{Ba}, and D_{Zn} may be reduced by 50% or more in the severely undersaturated abyssal Indo-Pacific [*McCorkle et al.*, 1995; *Marchitto et al.*, 2000, 2005]. Limited measurements on recently living (Rose Bengal-stained) foraminifera, laboratory dissolution experiments, and theoretical biomineralization considerations implicate reduced trace metal incorporation during growth, rather than postmortem preferential dissolution [*Boyle*, 1988; *Elderfield et al.*, 1996; *Marchitto et al.*, 2000]. Benthic foraminifera are believed to be more chemically homogenous than planktonic foraminifera, and therefore not subject to the same dissolution artifacts [*Boyle and Rosenthal*, 1996]. For Cd the ΔCO_3^{2-} effect is limited to undersaturated waters, but D_{Ba} and D_{Zn} appear to be reduced in even mildly supersaturated waters.

[9] Past changes in deep sea saturation state may therefore overprint benthic foraminiferal trace metal records, especially in regions that are poorly saturated today. In the deep Pacific, where glacial-interglacial changes in deep circulation are believed to have been small, ΔCO_3^{2-} was probably the dominant control on Zn/Ca (and to a lesser extent Cd/Ca) records [*Marchitto et al.*, 2005]. In the North Atlantic, glacial intrusion of low-CO_3^{2-} AABW may have lowered D_{Zn} slightly, but D_{Cd} was not likely affected [*Marchitto et al.*, 2002]. It is possible that Cd/Ca records from the deep South Atlantic are overprinted by changes in saturation state, but paleo-CO_3^{2-} is difficult to estimate. $CaCO_3$ accumulation in a South Atlantic core currently bathed by AABW suggests better preservation during glacial intervals, with highest inferred CO_3^{2-} levels during glacial terminations [*Hodell et al.*, 2001]. Farther north within the South Atlantic, CO_3^{2-} changes were likely dominated by the waxing and waning of AABW. Tropical paleo-CO_3^{2-} records based on planktonic foraminiferal shell weights show dissolution events during Marine Isotope Stage (MIS) 5/4 glacial intensifications [*Broecker and Clark*, 2003]. However, attempts to use shell weights to reconstruct South Atlantic paleo-CO_3^{2-} have been hampered by the complicating effects of variable growth conditions and pore water dissolution [*Broecker and Clark*, 2004]. Paired Cd/Ca and Zn/Ca data could theoretically provide insight because of the different sensitivities of these proxies to ΔCO_3^{2-} [*Marchitto et al.*, 2000, 2005]. There is also some indication that Cd/Ca in the benthic species *Nutallides umbonifera* is immune to the saturation effect [*Boyle and Rosenthal*, 1996; *Mackensen*, 1997].

[10] An additional challenge arises from within-sample heterogeneity. *Boyle* [1995] noted that the Cd/Ca scatter between triplicate picks (~15–20 individuals each) from a sediment sample is more than double that derived from equivalent-sized splits of crushed and homogenized individuals. The pooled standard deviation of the former approach (± 0.023 μmol mol^{-1}) is similar to the average within-core scatter of the Cd/Ca measurements compiled here. This error is equivalent to about ± 0.08 nmol Cd per kg seawater (at maximum D_{Cd} of 2.9), which is relatively large compared to the modern whole-Atlantic gradient of ~0.5 nmol kg^{-1} (Figure 2). Hence our reconstructed meridional sections (section 5.1) contain considerable noise, and individual data points must be viewed with caution. Possible causes for heterogeneity include: bioturbational mixing of non-contemporaneous individuals; variable microhabitats, even within the same species; unknown factors such as age or growth rate that may affect Cd uptake; and sedimentary contamination.

Table 1. Compilation of Published Holocene and LGM Benthic Foraminiferal Cd_W Data[a]

Core	Lat., deg	Long., deg	Depth, m	Hol. Cd_W, nmol/kg	LGM Cd_W, nmol/kg	References
AII107-65	−32.03	−36.19	2795		0.44	1
AII107-131	−30.88	−38.05	2925		0.36	1
BOFS11K	55.19	−20.35	2004	0.39	0.25	2
BOFS14K	58.62	−19.44	1756	0.37	0.17	2
BOFS17K	58.00	−16.50	1150	0.54	0.23	2
BOFS28K	24	−22	4900	0.35	0.54	3
BOFS29K	20	−21	4000	0.31	0.54	3
BOFS31K	19	−20	3330	0.34	0.46	3
CHN82-4	41.72	−32.85	3427	0.27	0.42	1, 4
CHN82-11	42.38	−31.80	3209	0.22	0.43	1, 4
CHN82-15	43.37	−28.23	2153	0.32	0.21	1, 4
CHN82-20	43.50	−29.87	3070	0.26	0.36	1, 4
EN66-10	6.65	−21.90	3527	0.42	0.68	1
EN66-16	5.47	−21.13	3152	0.37	0.72	1
EN66-32	2.47	−19.73	5003	0.34	0.48	1
EN66-38	4.92	−20.50	2931	0.45	0.71	1
EN120-GGC1	33.67	−57.62	4450	0.25	0.71	5
IOS82-PC-SO1	42.38	−23.52	3540	0.29	0.47	1
KNR64-5	16.52	−74.80	1800	0.25	0.13	1, 5
KNR110-82	4.34	−43.49	2816		0.32	1
KNR159-5-36	−27.51	−46.47	1268	0.50	0.40	6
M12328	21	−19	2778	0.29	0.42	3
M12392	25.17	−16.83	2573		0.30	1
M16004	29.98	−10.65	1512	0.22	0.30	7
M23414	53.54	−20.29	2196	0.37	0.40	7
M35003	12.08	−61.25	1299	0.47	0.30	8
NEAP-3K	62.83	−23.95	1510		0.21	9
NEAP-4K	61.48	−24.17	1627	0.35	0.28	9, 10
NEAP-8K	59.78	−23.90	2360		0.49	9
NEAP-15K	56.35	−27.80	2848		0.49	9
NEAP-17K/18B	54.68	−28.35	2880	0.34	0.40	9
NEAP-18K/19B	52.75	−30.33	3275	0.33	0.58	9
OC205-2-7JPC	26.14	−77.74	1320	0.37	0.19	11
OC205-2-33GGC	26.22	−77.69	783	0.37	0.17	11
OC205-2-103GGC	26.07	−78.06	965	0.35	0.16	11
OC205-2-106GGC	25.98	−78.18	654	0.39	0.25	11
OC205-2-108GGC	25.98	−78.18	743	0.39	0.20	11
OC205-2-149JPC	26.26	−77.67	423	0.17	0.15	11
ODP 980	55.48	−14.70	2168		0.24	4
RC12-267	−38.68	−25.78	4144	0.52	0.42	1
RC12-294	−37.27	−10.10	3308	0.44	0.51	1, 12
RC13-228	−22.33	11.20	3204	0.34	0.36	1, 12
RC13-229	−25.50	11.33	4191	0.49	0.50	1, 13, 14
RC16-84	−26.70	−43.33	2438	0.21	0.47	15
RC16-85	−29.92	−43.42	3909	0.69	0.70	15
RC16-86	−32.17	−43.93	3759	0.63	0.59	15
RC16-119	−27.70	−46.52	1567	0.41	0.29	15
SO75-26KL	37.82	−9.50	1099	0.36	0.19	7
SO82-05	59.19	−30.91	1416	0.67[b]	0.35[b]	7
V19-240	−30.58	−13.28	3103		0.56	1
V22-174	−10.07	−12.82	2630	0.34	0.36	1
V22-197	14.17	−18.58	3167	0.39	0.39	1
V23-100	22.68	−21.30	4579		0.52	1
V24-1	30.50	−73.50	3012		0.25	1
V24-253	−26.95	−44.68	2069	0.24	0.42	15
V25-59	1.37	−39.48	3824	0.26	0.45	1, 12
V26-176	36.00	−72.00	3942		0.32	1
V28-14	64.78	−29.57	1855		0.24	1
V28-73	57.18	−20.87	2063	0.57	0.30	4
V29-179	44.00	−24.53	3331	0.31	0.37	1
V29-193	55.40	−18.73	1326	0.50	0.28	4
V29-202	60.38	−20.97	2658	0.31	0.38	4

Table 1. (continued)

Core	Lat., deg	Long., deg	Depth, m	Hol. Cd_W, nmol/kg	LGM Cd_W, nmol/kg	References
V29-204	61.18	−23.02	1849	0.22	0.20	4
V30-40	0.20	−23.13	3706		0.52	1
V30-49	18.43	−21.08	3093	0.25	0.56	1, 16
V30-51	19.87	−19.92	3409	0.35	0.47	1
V30-97	41.00	−33.93	3371		0.34	1

[a] References: (1) *Boyle* [1992]; (2) *Bertram et al.* [1995]; (3) *Beveridge et al.* [1995]; (4) *Marchitto et al.* [2002]; (5) *Boyle and Keigwin* [1987]; (6) *Came et al.* [2003]; (7) *Willamowski and Zahn* [2000]; (8) *Zahn and Stüber* [2002]; (9) *Rickaby et al.* [2000]; (10) *Rickaby and Elderfield* [2005]; (11) *Marchitto et al.* [1998]; (12) *Rosenthal et al.* [1997]; (13) *Oppo and Rosenthal* [1996]; (14) *Lea* [1995]; (15) *Oppo and Horowitz* [2000]; and (16) *Martin and Lea* [1998].
[b] SO82-05 data not included in meridional sections because of very anomalous Holocene value.

[11] Finally, we cannot rule out analytical offsets between the various labs whose work is compiled here. At least three different cleaning protocols are represented: the original oxidative and reductive cleaning method developed for Cd/Ca [*Boyle and Keigwin*, 1985/1986]; a revised method that reverses the reductive and oxidative steps to better remove CdS overgrowths [*Boyle and Rosenthal*, 1996]; and a method developed for Ba/Ca that adds a DPTA step to dissolve sedimentary barite [*Lea and Boyle*, 1990]. We follow *Rosenthal et al.* [1997] in updating some early measurements [*Boyle*, 1992] that appear to be affected by CdS contamination. Published analyses were performed primarily by atomic absorption spectrophotometry (AAS) [*Boyle and Keigwin*, 1985/1986], but also by inductively coupled plasma mass spectrometry (ICP-MS) [*Lea and Martin*, 1996] and thermal ionization mass spectrometry (TIMS) [*Rickaby et al.*, 2000]. Interlaboratory calibration for Cd/Ca has generally been informal, and there is currently no community-wide standard available for this purpose.

4. Methods

[12] We have compiled published benthic foraminiferal Cd/Ca data from all Atlantic sediment cores that include measurements from the Last Glacial Maximum (LGM, ~20 kyr BP) (Table 1). The definition of LGM may vary slightly from study to study, but usually corresponds to near-maximum benthic $\delta^{18}O$ values [see, e.g., *Boyle*, 1992]. Some samples may span a few thousand years before and after 20 kyr BP. Combined with bioturbational mixing and the rather low sedimentation rates typical of the deep sea, this means that LGM values may incorporate foraminifera from more extreme intervals like Heinrich event 1, during which the formation of NADW/GNAIW may have ceased [*McManus et al.*, 2004]. Some high-resolution records show very elevated Cd/Ca during Heinrich event 1 [*Willamowski and Zahn*, 2000; *Zahn and Stüber*, 2002; *Rickaby and Elderfield*, 2005] and we avoid those measurements here. Some other cores may be so heavily bioturbated that LGM measurements include foraminifera from the Holocene and/or MIS 3.

[13] We also compile Holocene data, but only from the cores with LGM measurements. The definition of Holocene is even looser than that of the LGM. In some studies the reported Holocene values are only from core tops, which vary in age due to issues of core recovery and sedimentation. Other studies attempt to report late Holocene means, the true ages of which again vary with core quality.

[14] We include data from various benthic foraminiferal taxa as reported in the literature to allow for

Table 2. New Benthic Foraminiferal Cd_W Data

Core	Lat., deg	Long., deg	Depth, m	Hol. Cd_W, nmol/kg	LGM Cd_W, nmol/kg
OC205-2-97JPC	26.94	−77.85	1183	0.32	0.25
OC205-2-100GGC	26.06	−78.03	1057	0.36	0.28
RC8-19	−24.29	−14.70	3636		0.37
RC12-292	−39.68	−15.48	3541		0.54
RC13-188	1.82	−33.68	3451		0.57
RC24-10	−2.18	−11.25	3451		0.59
V22-26	8.72	−41.25	3720		0.70
V22-175	−8.77	−14.28	2950		0.51
V26-17	29.93	−45.08	3623		0.43

maximum spatial coverage. The dominant genera represented are *Cibicidoides*, *Uvigerina*, *Nutallides*, and *Hoeglundina*. In all cases we convert Cd/Ca to Cd_W (inferred paleo-seawater Cd concentration, in nmol kg^{-1}) using the depth-dependent calcitic partition coefficients from *Boyle* [1992] or the aragonitic *Hoeglundina* partition coefficient from *Boyle et al.* [1995]. Cd_W is therefore recalculated from studies that use "empirical" or "local" partition coefficients [*Bertram et al.*, 1995; *Willamowski and Zahn*, 2000]. The average error on individual Cd_W values, based only on Cd/Ca reproducibility, is estimated to be ±0.08 nmol kg^{-1} (±1σ).

[15] In addition to published data, we report unpublished data from two Little Bahama Bank cores and new data from seven Mid-Atlantic Ridge cores (Table 2). The Little Bahama Bank measurements (cruise OC205-2) were made by AAS at the Woods Hole Oceanographic Institution following the methods of *Marchitto et al.* [1998] except that several different taxa were employed (*H. elegans*, *C. kullenbergi*, *C. wuellerstorfi*, and *U. peregrina*). The new Mid-Atlantic Ridge measurements were made at the University of Colorado on ~10–15 individuals of *C. wuellerstorfi* (>250 μm) each, oxidatively and reductively cleaned following the methods of *Boyle and Keigwin* [1985/6] as modified by *Boyle and Rosenthal* [1996]. LGM intervals were identified using a combination of unpublished radiocarbon dates and percent $CaCO_3$ stratigraphies. Multiple trace metals were measured on a Thermo-Finnigan Element2 sector field single-collector ICP-MS using methods adapted from *Rosenthal et al.* [1999] [*Marchitto*, 2006]. Long-term 1σ precision for Cd/Ca is 1.8% across a wide range of Cd/Ca values and sample sizes. Elemental measures of diagenetic (Mn/Ca) and sedimentary (Fe/Ca) contamination were low, ranging from 11 to 68 μmol mol^{-1} and 4 to 51 μmol mol^{-1}, respectively.

[16] We have also compiled *Cibicidoides* $\delta^{13}C$ data, where available, from the cores used for Cd/Ca (Table 3). We limit the compilation to *Cibicidoides* because this epifaunal genus is commonly considered to be the most reliable recorder of seawater $\delta^{13}C$ [e.g., *Duplessy et al.*, 1984; *Curry and Oppo*, 2005]. We combine the $\delta^{13}C$ data with Cd_W to calculate $\delta^{13}C_{as}$ as described in section 5.2.

[17] We present meridional sections of Atlantic Cd_W and $\delta^{13}C_{as}$ constructed using the program Ocean Data View (R. Schlitzer, Ocean Data View, 2005; http://odv.awi-bremerhaven.de). Our contour

Table 3. *Cibicidoides* $\delta^{13}C$ With $\delta^{13}C_{as}$ Calculated From Cd_W Data in Tables 1 and 2[a]

Core	Hol. $\delta^{13}C$	LGM $\delta^{13}C$	Hol. $\delta^{13}C_{as}$	LGM $\delta^{13}C_{as}$
AII107-131	0.95	0.85		0.25
BOFS11K	1.43	1.40	0.51	0.49
BOFS14K	1.02	1.40	0.03	0.13
BOFS17K	1.03	1.61	0.51	0.61
BOFS28K	0.98	0.01	−0.05	−0.16
BOFS29K	0.82	0.00	−0.32	−0.17
BOFS31K	0.96	0.22	−0.11	−0.14
CHN82-4	1.11	0.48	−0.15	0.02
CHN82-11	1.17	0.66	−0.39	0.23
CHN82-15	0.96	1.21	−0.16	0.14
CHN82-20	1.30	0.76	0.00	0.15
EN66-10	0.82	0.19	−0.02	0.35
EN66-16	0.94	0.43	−0.04	0.68
EN66-32	0.86	−0.32	−0.21	−0.64
EN66-38	0.98	0.69	0.22	0.92
EN120-GGC1	0.33	−0.41	−1.05	−0.19
IOS82-PC-SO1	0.76	0.44	−0.44	0.10
KNR64-5	0.89	1.31	−0.48	−0.16
KNR110-82	1.11	0.21		−0.49
KNR159-5-36GGC	1.14	0.56	0.65	0.05
M12328	0.92	0.27	−0.29	−0.19
M12392	0.96	0.36		−0.39
M16004	1.03	1.10	−0.49	0.36
M23414	1.12	1.00	0.13	0.50
M35003	0.98	1.55	0.27	0.80
NEAP-4K	1.50	1.50	0.46	0.70
OC205-2-7JPC	1.30	1.37	0.32	0.19
OC205-2-33GGC	1.02	1.55	0.04	0.28
OC205-2-97JPC	1.23	1.53	0.12	0.62
OC205-2-100GGC	1.40	1.50	0.40	0.71
OC205-2-103GGC	1.27	1.56	0.23	0.24
OC205-2-106GGC	1.19	1.67	0.26	0.76
OC205-2-108GGC	1.14	1.71	0.21	0.57
OC205-2-149JPC	1.68	1.82	−0.12	0.46
ODP 980	1.04	0.82		−0.14
RC12-294	0.81	−0.23	0.02	−0.48
RC13-228	0.50	−0.31	−0.57	−0.92
RC13-229	0.39	−0.36	−0.27	−0.62
RC16-84	1.08	0.56	−0.51	0.22
RC16-119	1.10	0.99	0.23	0.22
SO75-26KL	1.02	1.60	0.01	0.43
SO82-05	1.35	1.60	1.20	0.96
V19-240		0.02		−0.11
V22-174	0.80	0.72	−0.27	0.12
V22-197	0.49	0.17	−0.44	−0.36
V23-100		0.00		−0.23
V24-253	1.10	0.48	−0.33	0.02
V25-59	1.03	0.07	−0.29	−0.32
V26-176		0.18		−0.52
V28-14	1.12	1.13		0.18
V28-73	1.17	1.16	0.74	0.41
V29-179	1.10	0.63	−0.05	0.05
V29-193	1.12	1.50	0.49	0.71
V29-202	1.06	0.45	−0.10	−0.11
V29-204	1.24	1.37	−0.32	0.23
V30-40		−0.11		−0.34
V30-49		0.21		0.07

[a] References given in Table 1.

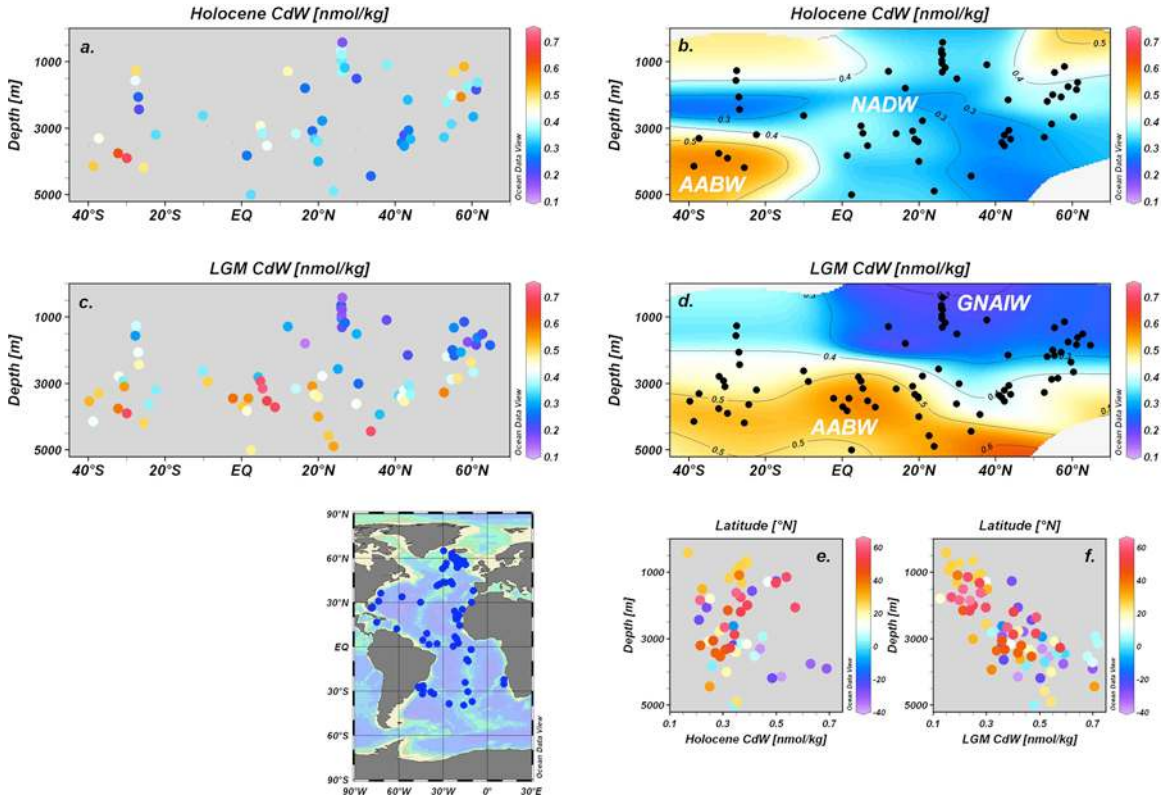

Figure 3. Meridional sections of inferred seawater dissolved Cd (Cd_W) for the (a and b) Holocene and (c and d) LGM Atlantic Ocean (see map for core distribution). Also shown are composite vertical profiles for the (e) Holocene and (f) LGM where colors indicate core latitude.

plots employ a relatively strong smoothing function (held constant between plots) to minimize the impact of anomalous cores. For Cd_W, individual values are also plotted for comparison with the smoothed plots. Only one core from the compilation (SO82-05) is not plotted due to its extremely anomalous Holocene Cd/Ca value. We present Cd_W sections that include all Atlantic data (Figure 3) as well as comparisons of the western and eastern basins (Figure 4). The western and eastern sections each include several cores from the crest of the Mid-Atlantic Ridge and all cores

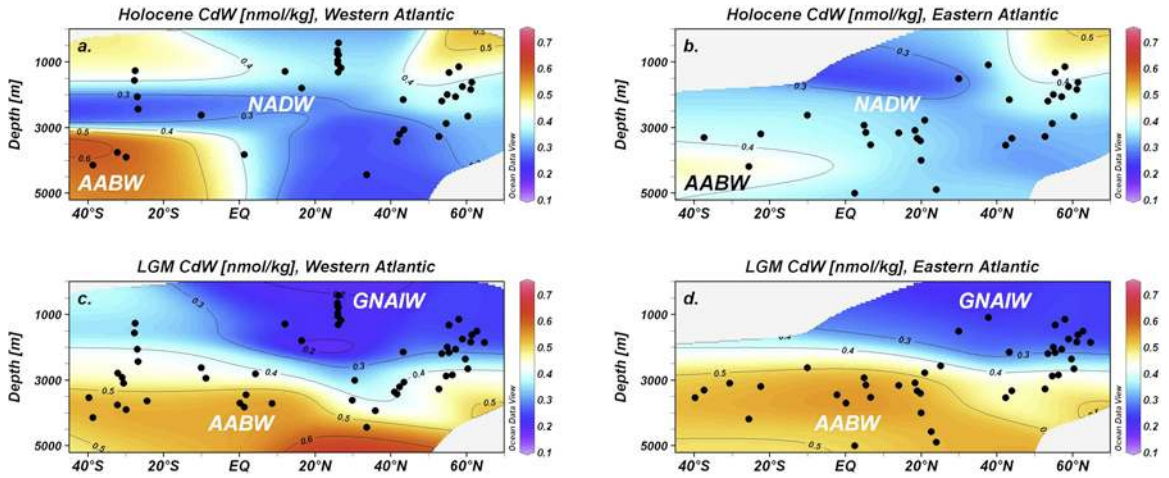

Figure 4. Meridional sections of Cd_W as in Figure 3 except separating (a and c) the western basins from (b and d) the eastern basins.

north of 50°N, most of which are from the eastern side of the Mid-Atlantic Ridge. No depth correction is made to the LGM data to account for lowered sea level.

5. LGM Atlantic Summary

5.1. Meridional Cd Sections

[18] Major syntheses of benthic foraminiferal Cd/Ca data for the LGM Atlantic have been performed by *Boyle* [1992], *Rosenthal et al.* [1997], and *Oppo and Horowitz* [2000]. Of these, only *Rosenthal et al.* [1997] presented a meridional section of glacial seawater Cd, following the approach that *Duplessy et al.* [1988] used for $\delta^{13}C$. We repeat that exercise here, incorporating new data that have appeared in the interim. Our LGM composite section contains data from 75 core locations, compared to *Rosenthal et al.*'s [1997] 19. Our main observations are broadly consistent with those of the earlier studies, with significant refinement afforded by the additional data.

[19] Before interpreting the LGM Cd_W sections, it is instructive to examine the Holocene sections to see how well Holocene foraminifera reproduce the modern Cd distribution. The nutrient pattern of the South Atlantic is captured reasonably well in the composite section (Figures 3a and 3b), with low-Cd NADW sandwiched between high-Cd AABW below and AAIW above. The volume of NADW expands to the north, as expected, with low-nutrient waters filling the entire water column by ~30°N. However, intermediate to mid-depth cores in the high-latitude North Atlantic tend to exhibit anomalously high Cd/Ca values. This problem is locally pervasive but not ubiquitous, and its cause is not known. *Bertram et al.* [1995] chose to use elevated empirical partition coefficients in this region based on core top Cd/Ca values, but as discussed above (section 4) we use the global partition coefficients of *Boyle* [1992]. The western Holocene section (Figure 4a) is similar to the composite, but the eastern section (Figure 4b) shows a weaker north-south deep Cd_W gradient. Reconstructed low to midlatitude deep North Atlantic waters contain more Cd in the east than in the west, while the opposite is true in the deep South Atlantic. Although these observations may be biased by sparse coverage, the North Atlantic data are consistent with the modern distribution of nutrients. Concentrations are lower in the better-ventilated deep western boundary current of NADW and higher in the northeastern basin, where deep recirculation is important for trapping nutrients [*Broecker et al.*, 1991].

[20] The composite LGM section is fundamentally different from the Holocene distribution, with NADW being replaced by low-Cd GNAIW lying above an expanded AABW (Figures 3c and 3d). This pattern is consistent with previous observations from Cd/Ca and $\delta^{13}C$ [e.g., *Boyle and Keigwin*, 1987; *Oppo and Fairbanks*, 1987; *Duplessy et al.*, 1988; *Boyle*, 1992; *Oppo and Lehman*, 1993; *Curry and Oppo*, 2005]. The boundary level between GNAIW and AABW appears to have been very sharp, occurring between ~2200 and 2500 m modern depth. The abruptness of this boundary and the dichotomy between the two water masses is well illustrated by the LGM depth profile (Figure 3f). The recent western Atlantic $\delta^{13}C$ compilation by *Curry and Oppo* [2005] also shows the sharpest vertical gradient between ~2000 and 2500 m. The relatively modest LGM Cd_W values found in the deepest Atlantic cores may suggest a slight depression of D_{Cd} by low-CO_3^{2-} AABW, but not by enough to obscure the accompanying rise in seawater Cd. The current lack of data poleward of 40°S prevents the accurate characterization of the AABW end-member, but we address this below using paired Cd and $\delta^{13}C$ (section 5.2). Data coverage in the intermediate depth South Atlantic is too sparse to infer the glacial presence or absence of AAIW. The deep (>3000 m) east-west Cd_W contrast during the LGM appears to have been weaker than during the Holocene, though there was perhaps a slightly deeper penetration of GNAIW in the west (Figures 4c and 4d). A reduced deep zonal contrast likely resulted from a combination of the loss of NADW and the spilling of AABW over the Walvis and Mid-Atlantic Ridges into the eastern basins [*Beveridge et al.*, 1995]. Comparison of western [*Curry and Oppo*, 2005] and eastern [*Sarnthein et al.*, 1994] sections of $\delta^{13}C$ at the LGM also suggest relatively little zonal contrast below ~3000 m.

5.2. Air-Sea $\delta^{13}C$

[21] The distributions of Cd and the $\delta^{13}C$ of dissolved inorganic carbon (DIC) are influenced by similar biological cycling, but $\delta^{13}C$ is also strongly impacted by air-sea exchange. If biological cycling were the only process acting on $\delta^{13}C$, it would decrease by about 1.1‰ for each 1 μmol kg^{-1} increase in dissolved phosphate, and a modern

oceanic range of ~3.3‰ would be possible [*Broecker and Maier-Reimer*, 1992]. However, air-sea exchange of CO_2 can isotopically enrich the DIC pool (increase $\delta^{13}C$), with greater enrichment in cases of (1) greater exchange due to long air-sea contact time or high winds; (2) exchange at colder temperatures; or (3) net CO_2 efflux out of the ocean into the atmosphere [*Mook et al.*, 1974; *Lynch-Stieglitz et al.*, 1995]. The net effect of the various air-sea exchange processes spans a modern surface ocean range of ~2‰.

[22] The air-sea component of $\delta^{13}C$ can be isolated by normalizing to zero phosphate, thus removing the biological component. *Broecker and Maier-Reimer* [1992] derived an equation for $\Delta\delta^{13}C$, later renamed $\delta^{13}C_{as}$ by *Lynch-Stieglitz and Fairbanks* [1994]:

$$\delta^{13}C_{as} = \delta^{13}C + 1.1P - 2.7 \quad (5)$$

where 2.7 is an arbitrary constant introduced to bring deep Pacific and Indian Ocean waters close to zero. $\delta^{13}C_{as}$ is a conservative tracer of deep waters because once a parcel of water leaves the surface ocean, its $\delta^{13}C_{as}$ signature is only altered by mixing [*Lynch-Stieglitz and Fairbanks*, 1994]. $\delta^{13}C_{as}$ can therefore be used to separate mixing and biogeochemical aging processes. Modern NADW is characterized by negative $\delta^{13}C_{as}$ values, while AABW and AAIW have positive signatures. AAIW is especially enriched in $\delta^{13}C_{as}$ due to formation from surface waters that are partially equilibrated with the atmosphere at cold temperatures [*Charles and Fairbanks*, 1990; *Charles et al.*, 1993].

[23] Following the example of *Oppo and Fairbanks* [1989], *Lynch-Stieglitz and Fairbanks* [1994] proposed that paleo-$\delta^{13}C_{as}$ can be estimated by using phosphate estimates derived from Cd/Ca. They combined equation (5) with the global Cd:phosphate relationship of *Boyle* [1988] (for P > 1.34 μmol kg^{-1}; equation (3)) to give an equation for Holocene deep ocean $\delta^{13}C_{as}$:

$$\delta^{13}C_{as} = \delta^{13}C + 2.75Cd - 2.0 \quad (6)$$

Lynch-Stieglitz et al. [1996] noted that during the LGM, organic matter $\delta^{13}C$ was ~2‰ higher [*Rau et al.*, 1991] and mean ocean $\delta^{13}C$ was ~0.3‰ lower [*Duplessy et al.*, 1988], so the relationship between $\delta^{13}C$ and phosphate was slightly different. Taking this into account and assuming unchanged oceanic Cd and phosphate inventories, they derived the following equation for $\delta^{13}C_{as}$ in the LGM deep ocean (P > 1.34 μmol kg^{-1}):

$$\delta^{13}C_{as} = \delta^{13}C + 2.375Cd - 1.46 \quad (7)$$

Two additional equations can be derived for waters with (P < 1.34 μmol kg^{-1}):

$$\delta^{13}C_{as} = \delta^{13}C + 5.29Cd - 2.7 \text{ (Holocene)} \quad (8)$$

$$\delta^{13}C_{as} = \delta^{13}C + 4.57Cd - 2.05 \text{ (LGM)} \quad (9)$$

[24] We use *Cibicidoides* $\delta^{13}C$ (where available) from our compiled Atlantic Cd/Ca sites to calculate $\delta^{13}C_{as}$ during the Holocene and LGM, using equations (6)–(9) (Table 3). It must be noted that the resulting Holocene meridional section of $\delta^{13}C_{as}$ bears relatively little resemblance to its modern distribution (Figure 5a). Although NADW below ~2000 m displays negative values and AAIW appears to be positive (both as expected), upper North Atlantic values are generally too positive and there is no sign of a positive AABW. The upper North Atlantic anomaly is related, at least in part, to the anomalously high Holocene Cd/Ca values found in this region, as noted above. The paucity of paired Cd:$\delta^{13}C$ data in the deep South Atlantic may hinder the proper reconstruction of AABW $\delta^{13}C_{as}$.

[25] Given the problems with the Holocene reconstruction, the LGM $\delta^{13}C_{as}$ section (Figure 5b) should be viewed with some caution. Nevertheless, some interesting patterns emerge. As in previous reconstructions [*Lynch-Stieglitz and Fairbanks*, 1994; *Oppo and Horowitz*, 2000] GNAIW is clearly characterized by positive $\delta^{13}C_{as}$ values, compared to ~−0.4 to −0.6‰ for modern NADW [*Charles et al.*, 1993; *Lynch-Stieglitz et al.*, 1995]. The deep South Atlantic, in contrast, had a negative $\delta^{13}C_{as}$ signature instead of the slightly positive values of modern AABW. It has long been noted that South Atlantic Cd/Ca shows little to no glacial-interglacial change while $\delta^{13}C$ was much lower during the LGM, resulting in low $\delta^{13}C_{as}$ [*Boyle*, 1992; *Boyle and Rosenthal*, 1996; *Rosenthal et al.*, 1997]. Although some very low Southern Ocean $\delta^{13}C$ values have been questioned because of microhabitat effects caused by high fluxes of algal detritus [*Mackensen et al.*, 1993], the spatial uniformity of Southern Ocean $\delta^{13}C$ during the LGM argues for a real drop in deep water values [*Ninnemann and Charles*, 2002]. As noted above, deep South Atlantic Cd/Ca may hypothetically have been affected by decreased seawater CO_3^{2-}

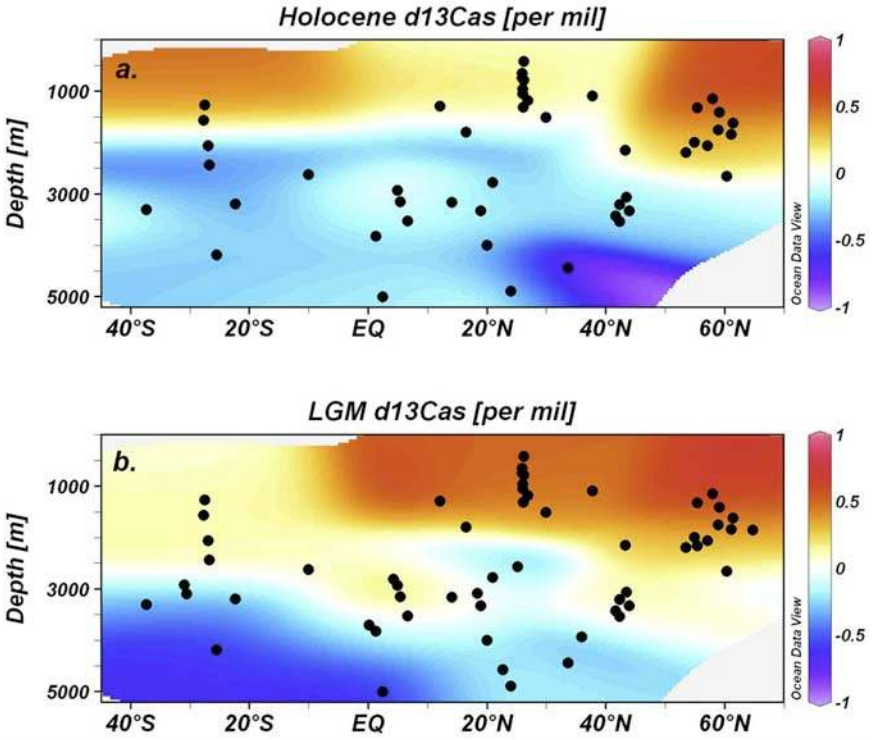

Figure 5. Meridional sections of $\delta^{13}C_{as}$ calculated from benthic foraminiferal Cd/Ca and $\delta^{13}C$ for the (a) Holocene and (b) LGM Atlantic Ocean.

during the LGM, but the magnitude of this effect is difficult to estimate.

[26] The glacial expansion of AABW allows for better $\delta^{13}C_{as}$ characterization of this water mass than in the Holocene section, yet we still have no data from the Southern Ocean poleward of 40°S. However, we can use a $\delta^{13}C$:Cd_W cross-plot to extrapolate to an AABW end-member estimate for the LGM (Figure 6). The $\delta^{13}C$:Cd_W plot allows for the separation of biogeochemical aging (along lines of constant $\delta^{13}C_{as}$) from mixing of water masses with different $\delta^{13}C_{as}$ signatures (across lines of constant $\delta^{13}C_{as}$). The LGM Atlantic data can largely be explained by mixing between high-$\delta^{13}C_{as}$ GNAIW and low-$\delta^{13}C_{as}$ AABW. Deep North Atlantic data fall between these two end-members, suggesting some mixing across the bathyal nutricline at ~2200 to 2500 m. *Ninnemann and Charles* [2002] reconstructed uniform LGM AABW values of ~−0.8‰ in the Atlantic sector of the Southern Ocean. Extrapolating the mixing line to this value suggests that the AABW end-member had a Cd concentration of roughly 0.6 to 0.8 nmol kg^{-1} and a $\delta^{13}C_{as}$ signature of perhaps −0.5 to −1‰. The implication of this analysis is that much of the $\delta^{13}C$ depletion in glacial AABW was due to

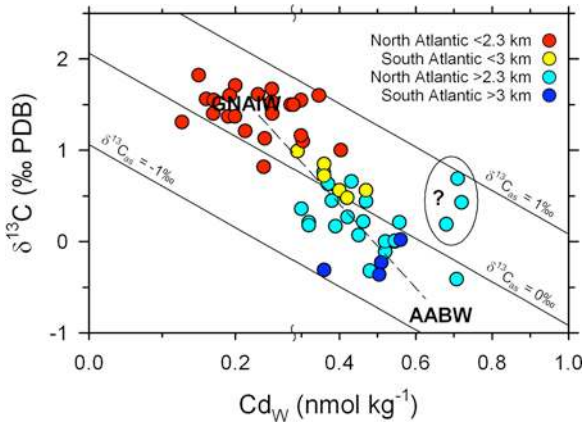

Figure 6. LGM $\delta^{13}C$ and Cd_W data from the Atlantic Ocean, with lines of constant $\delta^{13}C_{as}$. Note scale change on the Cd_W axis, which produces straight $\delta^{13}C_{as}$ isolines from two different $\delta^{13}C_{as}$ equations (equations (7) and (9)) and therefore better illustrates water mass mixing and biogeochemical aging. AABW placement is based on extending dashed mixing line to a $\delta^{13}C$ value of −0.8‰ [*Ninnemann and Charles*, 2002]. Three sites inside oval fall significantly off of the mixing line between high-$\delta^{13}C_{as}$ GNAIW and low-$\delta^{13}C_{as}$ AABW. These sites are from Sierra Leone Rise in the eastern tropical North Atlantic [*Boyle*, 1992] and are not easily explained by mixing or aging of other waters.

altered air-sea processes. Widespread microhabitat [*Mackensen et al.*, 1993] or CO_3^{2-} effects [*McCorkle et al.*, 1995] are not required to explain the distribution of $\delta^{13}C$:Cd_W data in Figure 6.

[27] Although there are no LGM $\delta^{13}C_{as}$ data from the modern core region of AAIW, we note that upper South Atlantic values are generally lower than in GNAIW (Figures 5b and 6). This pattern could be explained by simple mixing between GNAIW and AABW, but we cannot rule out the existence of a negative-$\delta^{13}C_{as}$ AAIW during the LGM.

6. Discussion

[28] Most theories put forward to explain the deep water configuration of the LGM Atlantic have relied on changes in buoyancy forcing in the high latitude North Atlantic. That is, fresher and therefore less dense surface waters in the North Atlantic reduced the formation rate and/or penetration depth of NADW/GNAIW [e.g., *Weyl*, 1968; *Broecker et al.*, 1985; *Boyle and Keigwin*, 1987]. Ocean circulation models suggest that reduced sea surface salinities and greater sea ice cover in the glacial North Atlantic could cause not only a shallower mode of deep water production, but also a shift in its production site to south of the Nordic Seas [*Rahmstorf*, 1994, 2002; *Ganopolski et al.*, 1998]. Such a change in deep convection sites would reduce ocean heat transport to higher latitudes, even if the rate of NADW/GNAIW production was unchanged. Alternatively, reduced production rates in the north may have been balanced by increased rates of AABW production in the south [*Broecker*, 1998]. Although the question of rate cannot be addressed with paleonutrient data alone [*LeGrand and Wunsch*, 1995], the sharp mid-depth nutricline reconstructed here argues for a significantly altered mode of circulation during the LGM.

[29] It is also possible that surface processes in the Southern Ocean were mainly responsible for the LGM circulation pattern. Longstanding theories of the modern MOC require that deep waters return to the surface by vertical mixing through the thermocline [*Stommel*, 1958; *Stommel and Arons*, 1960]. The magnitude of this mixing, which derives its energy from winds and tides, may ultimately determine the global rate of deep water formation [*Munk and Wunsch*, 1998]. *Toggweiler and Samuels* [1995, 1998] argue that much of the modern mixing occurs not across the thermocline but in the Southern Ocean, where circumpolar westerlies blowing over the latitude band of Drake Passage force northward Ekman drift that is balanced by deep upwelling. This upwelling, combined with adequately dense surface waters in the North Atlantic, may set the southward flux of NADW. Today net precipitation over the Southern Ocean allows for the buoyant conversion of NADW into AAIW. *Keeling and Stephens* [2001] hypothesized that during the LGM, deep water temperatures approached the freezing point, so exposure to the Southern Ocean surface resulted in extensive sea ice cover. This sea ice shielded deep waters from precipitation, retarding the buoyant conversion of NADW. Salt became concentrated in AABW and AAIW such that both theoretically became denser than NADW/GNAIW. The upper depth limit of AABW would then correspond to the lower limit of AAIW, which is set by the depth of the seafloor ridges crossing the latitudes of Drake Passage; below this depth topographic boundaries would cause southward geostrophic recirculation of AAIW. *Warren* [1990] estimated the relevant ridge depth to lie between ~1500 and 2500 m, which spans the GNAIW-AABW Cd nutricline (~2200–2500 m) reconstructed here.

[30] Glacial pore water $\delta^{18}O$ measurements, combined with benthic foraminiferal $\delta^{18}O$, suggest that the deep ocean was more homogenously cold than today, very close to the freezing point of seawater [*Adkins et al.*, 2002; *Schrag et al.*, 2002]. Pore water chlorinity further suggests that glacial AABW within the Southern Ocean was much saltier and therefore much denser than deep waters in the North Atlantic [*Adkins et al.*, 2002]. Such a reversal of the meridional salinity gradient (modern AABW is fresher than NADW) could be explained by glacial AABW formation by brine rejection beneath extensive sea ice [*Adkins et al.*, 2002]. This scenario is broadly consistent with the *Keeling and Stephens* [2001] hypothesis of filling the deep Atlantic with dense Southern Ocean waters. However, it is not clear how well the pore water evidence for dense AABW coincides with the Cd and $\delta^{13}C$ reconstructions of widespread AABW: deep (4584 m) and mid-depth (2184 m) North Atlantic sites appear to have been equally less dense than AABW, with no clear evidence of a mixing gradient. Additional Atlantic pore water sites may be required to elucidate the glacial spreading of salty AABW.

[31] GNAIW likely acquired its high $\delta^{13}C_{as}$ signature through longer air-sea contact at cold temperatures [*Lynch-Stieglitz and Fairbanks*, 1994]. In

contrast, glacial AABW probably acquired its low $\delta^{13}C_{as}$ signature because of poor ventilation during its formation around Antarctica, with GNAIW not significantly contributing to its feed waters [*Ninnemann and Charles*, 2002; *Sigman et al.*, 2003]. In particular, AABW formation beneath sea ice [*Keeling and Stephens*, 2001; *Adkins et al.*, 2002] could have produced the observed negative $\delta^{13}C_{as}$ values. Reduced ventilation of the Southern Ocean is also an important mechanism in numerous models of glacial atmospheric CO_2 lowering [e.g., *Francois et al.*, 1997; *Toggweiler*, 1999; *Sigman and Boyle*, 2000; *Stephens and Keeling*, 2000; *Toggweiler et al.*, 2006].

7. Conclusions

[32] Benthic foraminiferal Cd/Ca and $\delta^{13}C$ both clearly support an LGM expansion of high-nutrient AABW and a replacement of low-nutrient NADW by the shallower GNAIW. Cd/Ca suggests that the main mixing boundary between AABW and GNAIW occurred abruptly between ~2200 and 2500 m modern water depth. Cd concentration differences between the western and eastern basins of the deep Atlantic may have been diminished during the LGM due to the spilling of AABW over mid-ocean ridges. Combined Cd and $\delta^{13}C$ data indicate that the entire glacial Atlantic can be characterized by mixing between high-$\delta^{13}C_{as}$ GNAIW and low-$\delta^{13}C_{as}$ AABW. Waters in the upper South Atlantic may alternately reflect mixing between GNAIW and a relatively low-$\delta^{13}C_{as}$ AAIW. Although we cannot determine whether conditions in the North Atlantic or Southern Ocean were more important for setting the LGM circulation pattern, it is apparent that both GNAIW and AABW formed under different conditions than their modern counterparts. In particular, low $\delta^{13}C_{as}$ suggests that AABW was more poorly ventilated than today, likely contributing to decreased atmospheric CO_2.

[33] Cd/Ca data coverage is sparsest in the tropical South Atlantic and the Southern Ocean, with no LGM values poleward of 40°S. Glacial Cd/Ca data from the Southern Ocean are needed to better define the end-member composition of AABW and to determine the status of AAIW. Paired Cd and $\delta^{13}C$ data from the upper South Atlantic would be valuable for determining the air-sea conditions that AAIW may have formed under. Improved understanding of benthic foraminiferal trace metal incorporation and potential artifacts is also warranted, especially in the high latitude North Atlantic where correspondence between core top Cd/Ca and modern seawater Cd is often poor. Laboratory culture work could be particularly valuable in this regard. Finally, numerical modeling of paleonutrient distributions is essential for exploring the dynamic and climatic implications of the data.

Acknowledgments

[34] This paper evolved from an invited presentation by Marchitto at the March 2005 SCOR/IMAGES Workshop on Past Ocean Circulation in Atlanta, organized by J. Lynch-Stieglitz and C. Kissel. We thank E. Clark and C. Wolak for laboratory assistance; R. Came, H. Elderfield, Y. Rosenthal, and R. Zahn for suggestions regarding compiled data; W. Curry and U. Ninnemann for insightful discussions; and C. Charles and an anonymous reviewer for comments that significantly improved this manuscript. *Oceanus* cores are curated at WHOI with support from NSF, ONR, and USGS, and *Robert Conrad* and *Vema* cores are curated at LDEO with support from NSF and ONR. This work was supported by NSF grant OCE-0221979 to Broecker, S. Hemming, J. Lynch-Stieglitz, and Marchitto.

References

Adkins, J. F., K. McIntyre, and D. P. Schrag (2002), The salinity, temperature, and $\delta^{18}O$ of the glacial deep ocean, *Science*, *298*, 1769–1773.

Bainbridge, A. E. (1981), *GEOSECS Atlantic Expedition, Vol. 1, Hydrographic Data*, U.S. Govt. Print. Off., Washington, D. C.

Behl, R. J., and J. P. Kennett (1996), Brief interstadial events in the Santa Barbara basin, NE Pacific, during the past 60 kyr, *Nature*, *379*, 243–246.

Bertram, C. J., H. Elderfield, N. J. Shackleton, and J. A. MacDonald (1995), Cadmium/calcium and carbon isotope reconstructions of the glacial northeast Atlantic Ocean, *Paleoceanography*, *10*, 563–578.

Beveridge, N. A. S., H. Elderfield, and N. J. Shackleton (1995), Deep thermohaline circulation in the low-latitude Atlantic during the last glacial, *Paleoceanography*, *10*, 643–660.

Boyle, E. A. (1988), Cadmium: Chemical tracer of deepwater paleoceanography, *Paleoceanography*, *3*, 471–489.

Boyle, E. A. (1992), Cadmium and $\delta^{13}C$ paleochemical ocean distributions during the stage 2 glacial maximum, *Annu. Rev. Earth Planet. Sci.*, *20*, 245–287.

Boyle, E. A. (1995), Limits on benthic foraminiferal chemical analyses as precise measures of environmental properties, *J. Foraminiferal Res.*, *25*, 4–13.

Boyle, E. A., and L. D. Keigwin (1982), Deep circulation of the North Atlantic over the last 200,000 years: Geochemical evidence, *Science*, *218*, 784–787.

Boyle, E. A., and L. D. Keigwin (1985/1986), Comparison of Atlantic and Pacific paleochemical records for the last 215,000 years: Changes in deep ocean circulation and chemical inventories, *Earth Planet. Sci. Lett.*, *76*, 135–150.

Boyle, E. A., and L. D. Keigwin (1987), North Atlantic thermohaline circulation during the past 20,000 years linked to high-latitude surface temperature, *Nature*, *330*, 35–40.

Boyle, E. A., and Y. Rosenthal (1996), Chemical hydrography of the South Atlantic during the last glacial maximum: Cd vs. $\delta^{13}C$, in *The South Atlantic: Present and Past Circulation*, edited by G. Wefer et al., pp. 423–443, Springer, New York.

Boyle, E. A., F. R. Sclater, and J. M. Edmond (1976), On the marine geochemistry of cadmium, *Nature*, *263*, 42–44.

Boyle, E. A., L. Labeyrie, and J. C. Duplessy (1995), Calcitic foraminiferal data confirmed by cadmium in aragonitic *Hoeglundina*: Application to the last glacial maximum in the northern Indian Ocean, *Paleoceanography*, *10*, 881–900.

Broecker, W. S. (1998), Paleocean circulation during the last deglaciation: A bipolar seesaw?, *Paleoceanography*, *13*(2), 119–121.

Broecker, W. S., and E. Clark (2003), $CaCO_3$ dissolution in the deep sea: Paced by insolation cycles, *Geochem. Geophys. Geosyst.*, *4*(7), 1059, doi:10.1029/2002GC000450.

Broecker, W. S., and E. Clark (2004), Shell weights from the South Atlantic, *Geochem. Geophys. Geosyst.*, *5*, Q03003, doi:10.1029/2003GC000625.

Broecker, W. S., and E. Maier-Reimer (1992), The influence of air and sea exchange on the carbon isotope distribution in the sea, *Global Biogeochemical. Cycles*, *6*, 315–320.

Broecker, W. S., and T.-H. Peng (1987), The role of $CaCO_3$ compensation in the glacial to interglacial atmospheric CO_2 change, *Global Biogeochem. Cycles*, *1*, 15–29.

Broecker, W. S., D. M. Peteet, and D. Rind (1985), Does the ocean-atmosphere system have more than one stable mode of operation?, *Nature*, *315*, 21–25.

Broecker, W. S., S. Blanton, W. M. Smethie, and G. Ostlund (1991), Radiocarbon decay and oxygen utilization in the deep Atlantic Ocean, *Global Biogeochem. Cycles*, *5*, 87–117.

Came, R. E., D. W. Oppo, and W. B. Curry (2003), Atlantic Ocean circulation during the Younger Dryas: Insights from a new Cd/Ca record from the western subtropical South Atlantic, *Paleoceanography*, *18*(4), 1086, doi:10.1029/2003PA000888.

Charles, C. D., and R. G. Fairbanks (1990), Glacial to interglacial changes in isotopic gradients of Southern Ocean water: Arctic versus Antarctic, in *Geological History of the Polar Oceans*, edited by U. Bleil and J. Thiede, pp. 519–538, Springer, New York.

Charles, C. D., J. D. Wright, and R. G. Fairbanks (1993), Thermodynamic influences on the marine carbon isotope record, *Paleoceanography*, *8*, 691–697.

Cullen, J. T., T. W. Lane, F. M. M. Morel, and R. M. Sherrell (1999), Modulation of cadmium uptake in phytoplankton by seawater CO_2 concentration, *Nature*, *402*, 165–167.

Curry, W. B., and D. W. Oppo (2005), Glacial water mass geometry and the distribution of $\delta^{13}C$ of ΣCO_2 in the western Atlantic Ocean, *Paleoceanography*, *20*, PA1017, doi:10.1029/2004PA001021.

Duplessy, J. C., N. J. Shackleton, R. K. Matthews, W. Prell, W. F. Ruddiman, M. Caralp, and C. H. Hendy (1984), $\delta^{13}C$ record of benthic foraminifera in the last interglacial ocean: Implications for the carbon cycle and the global deep water circulation, *Quat. Res.*, *21*, 225–243.

Duplessy, J. C., N. J. Shackleton, R. G. Fairbanks, L. Labeyrie, D. Oppo, and N. Kallel (1988), Deepwater source variations during the last climatic cycle and their impact on global deepwater circulation, *Paleoceanography*, *3*, 343–360.

Elderfield, H., and R. E. M. Rickaby (2000), Oceanic Cd/P ratio and nutrient utilization in the glacial Southern Ocean, *Nature*, *405*, 305–310.

Elderfield, H., C. J. Bertram, and J. Erez (1996), A biomineralization model for the incorporation of trace elements into foraminiferal calcium carbonate, *Earth Planet. Sci. Lett.*, *142*, 409–423.

Francois, R., M. A. Altabet, E.-F. Yu, D. M. Sigman, M. P. Bacon, M. Frank, G. Bohrmann, G. Bareille, and L. D. Labeyrie (1997), Contribution of Southern Ocean surface-water stratification to low atmospheric CO_2 concentrations during the last glacial period, *Nature*, *389*, 929–935.

Ganopolski, A., and S. Rahmstorf (2001), Rapid changes of glacial climate simulated in a coupled climate model, *Nature*, *409*, 153–158.

Ganopolski, A., S. Rahmstorf, V. Petoukhov, and M. Claussen (1998), Simulation of modern and glacial climates with a coupled global model of intermediate complexity, *Nature*, *391*, 351–356.

Hodell, D. A., C. D. Charles, and F. J. Sierro (2001), Late Pleistocene evolution of the ocean's carbonate system, *Earth Planet. Sci. Lett.*, *192*, 109–124.

Keeling, R. F., and B. B. Stephens (2001), Antarctic sea ice and the control of Pleistocene climate instability, *Paleoceanography*, *16*(1), 112–131.

Kroopnick, P. M. (1985), The distribution of ^{13}C of ΣCO_2 in the world oceans, *Deep Sea Res., Part A*, *32*, 57–84.

Lea, D. W. (1995), A trace metal perspective on the evolution of Antarctic Circumpolar Deep Water chemistry, *Paleoceanography*, *10*, 733–748.

Lea, D. W., and E. A. Boyle (1989), Barium content of benthic foraminifera controlled by bottom-water composition, *Nature*, *338*, 751–753.

Lea, D. W., and E. A. Boyle (1990), Foraminiferal reconstruction of barium distributions in water masses of the glacial oceans, *Paleoceanography*, *5*, 719–742.

Lea, D. W., and P. A. Martin (1996), A rapid mass spectrometric method for the simultaneous analysis of barium, cadmium, and strontium in foraminifera shells, *Geochim. Cosmochim. Acta*, *60*, 3143–3149.

LeGrand, P., and C. Wunsch (1995), Constraints from paleotracer data on the North Atlantic circulation during the last glacial maximum, *Paleoceanography*, *10*, 1011–1046.

Lynch-Stieglitz, J., and R. G. Fairbanks (1994), A conservative tracer for glacial ocean circulation from carbon isotope and palaeo-nutrient measurements in benthic foraminifera, *Nature*, *369*, 41–43.

Lynch-Stieglitz, J., T. F. Stocker, W. S. Broecker, and R. G. Fairbanks (1995), The influence of air-sea exchange on the isotopic composition of oceanic carbon: Observations and modeling, *Global Biogeochem. Cycles*, *9*, 653–665.

Lynch-Stieglitz, J., A. van Geen, and R. G. Fairbanks (1996), Interocean exchange of Glacial North Atlantic Intermediate Water: Evidence from Subantarctic Cd/Ca and $\delta^{13}C$ measurements, *Paleoceanography*, *11*, 191–201.

Mackensen, A. (1997), Foraminiferal proxies: Constraints on their use in high latitude paleoceanography, *Rep. Polar Res.*, *243*, 145 pp., Alfred Wegener Inst. for Pol. and Mar. Res., Bremerhaven, Germany.

Mackensen, A., H.-W. Hubberten, T. Bickert, G. Fischer, and D. K. Fütterer (1993), $\delta^{13}C$ in benthic foraminiferal tests of Fontabia wuellerstorfi (Schwager) relative to $\delta^{13}C$ of dissolved inorganic carbon in Southern Ocean deep water: Implications for Glacial ocean circulation models, *Paleoceanography*, *8*, 587–610.

Marchitto, T. M. (2004), Lack of a significant temperature influence on the incorporation of Cd into benthic foraminiferal tests, *Geochem. Geophys. Geosyst.*, *5*, Q10D11, doi:10.1029/2004GC000753.

Marchitto, T. M. (2006), Precise multielemental ratios in small foraminiferal samples determined by sector field ICP-MS,

Geochem. Geophys. Geosyst., *7*, Q05P13, doi:10.1029/2005GC001018.

Marchitto, T. M., W. B. Curry, and D. W. Oppo (1998), Millennial-scale changes in North Atlantic circulation since the last glaciation, *Nature*, *393*, 557–561.

Marchitto, T. M., W. B. Curry, and D. W. Oppo (2000), Zinc concentrations in benthic foraminifera reflect seawater chemistry, *Paleoceanography*, *15*, 299–306.

Marchitto, T. M., Jr., D. W. Oppo, and W. B. Curry (2002), Paired benthic foraminiferal Cd/Ca and Zn/Ca evidence for a greatly increased presence of Southern Ocean Water in the glacial North Atlantic, *Paleoceanography*, *17*(3), 1038, doi:10.1029/2000PA000598.

Marchitto, T. M., J. Lynch-Stieglitz, and S. R. Hemming (2005), Deep Pacific $CaCO_3$ compensation and glacial-interglacial atmospheric CO_2, *Earth Planet. Sci. Lett.*, *231*, 317–336.

Martin, P. A., and D. W. Lea (1998), Comparison of water mass changes in the deep tropical Atlantic derived from Cd/Ca and carbon isotope records: Implications for changing Ba composition of deep Atlantic water masses, *Paleoceanography*, *13*, 572–585.

McCorkle, D. C., P. A. Martin, D. W. Lea, and G. P. Klinkhammer (1995), Evidence of a dissolution effect on benthic foraminiferal shell chemistry: $\delta^{13}C$, Cd/Ca, Ba/Ca, and Sr/Ca results from the Ontong Java Plateau, *Paleoceanography*, *10*, 699–714.

McCorkle, D. C., B. H. Corliss, and C. A. Farnham (1997), Vertical distributions and stable isotopic compositions of live (stained) benthic foraminifera from the North Carolina and California continental margins, *Deep Sea Res.*, *Part I*, *44*, 983–1024.

McManus, J. F., R. Francois, J.-M. Gherardi, L. D. Keigwin, and S. Brown-Leger (2004), Collapse and rapid resumption of Atlantic meridional circulation linked to deglacial climate changes, *Nature*, *428*, 834–837.

Mook, W. G., J. C. Bommerson, and W. H. Staverman (1974), Carbon isotope fractionation between dissolved bicarbonate and gaseous carbon dioxide, *Earth Planet. Sci. Lett.*, *22*, 169–176.

Morel, F. M. M., A. J. Milligan, and M. A. Saito (2003), Marine bioinorganic chemistry: The role of trace metals in the oceanic cycles of major nutrients, in *Treatise on Geochemistry*, vol. 6, edited by H. Elderfield, H. D. Holland, and K. K. Turekian, pp. 113–143, Elsevier, New York.

Munk, W., and C. Wunsch (1998), Abyssal recipes - II. Energetics of tidal and wind mixing, *Deep Sea Res.*, *Part I*, *45*, 1977–2010.

Ninnemann, U. S., and C. D. Charles (2002), Changes in the mode of Southern Ocean circulation over the last glacial cycle revealed by foraminiferal stable isotopic variability, *Earth Planet. Sci. Lett.*, *201*, 383–396.

Nozaki, Y. (1997), A fresh look at element distribution in the North Pacific, *Eos Trans. AGU*, *78*, 221.

Oppo, D. W., and R. G. Fairbanks (1987), Variability in the deep and intermediate water circulation of the Atlantic Ocean during the past 25,000 years: Northern Hemisphere modulation of the Southern Ocean, *Earth Planet. Sci. Lett.*, *86*, 1–15.

Oppo, D. W., and R. G. Fairbanks (1989), Carbon isotope composition of tropical surface water during the past 22,000 years, *Paleoceanography*, *4*, 333–351.

Oppo, D. W., and M. Horowitz (2000), Glacial deep water geometry: South Atlantic benthic foraminiferal Cd/Ca and $\delta^{13}C$ evidence, *Paleoceanography*, *15*, 147–160.

Oppo, D. W., and S. J. Lehman (1993), Mid-depth circulation of the subpolar North Atlantic during the Last Glacial Maximum, *Science*, *259*, 1148–1152.

Oppo, D. W., and Y. Rosenthal (1996), Cd/Ca changes in a deep Cape Basin core over the past 730,000 years: Response of circumpolar deepwater variability to northern hemisphere ice sheet melting?, *Paleoceanography*, *9*, 661–675.

Ortiz, J. D., S. B. O'Connell, J. DelViscio, W. Dean, J. D. Carriquiry, T. M. Marchitto, Y. Zheng, and A. van Geen (2004), Enhanced marine productivity off western North America during warm climate intervals of the past 52 k. y., *Geology*, *32*, 521–524.

Peterson, L. C., G. H. Haug, K. A. Hughen, and U. Rohl (2000), Rapid changes in the hydrologic cycle of the tropical Atlantic during the last glacial, *Science*, *290*, 1947–1951.

Rahmstorf, S. (1994), Rapid climate transitions in a coupled ocean-atmosphere model, *Nature*, *372*, 82–85.

Rahmstorf, S. (2002), Ocean circulation and climate during the past 120,000 years, *Nature*, *419*, 207–214.

Rau, G. H., P. N. Froelich, T. Takahashi, and D. J. Des Marais (1991), Does sedimentary organic $\delta^{13}C$ record variations in Quaternary ocean $[CO_2(aq)]$?, *Paleoceanography*, *6*, 335–347.

Rickaby, R. E. M., and H. Elderfield (2005), Evidence from the high-latitude North Atlantic for variations in Antarctic Intermediate water flow during the last deglaciation, *Geochem. Geophys. Geosyst.*, *6*, Q05001, doi:10.1029/2004GC000858.

Rickaby, R. E. M., M. Greaves, and H. Elderfield (2000), Cd in planktonic and benthic foraminiferal shells determined by thermal ionisation mass spectrometry, *Geochim. Cosmochim. Acta*, *64*, 1229–1236.

Rosenthal, Y., E. A. Boyle, and L. Labeyrie (1997), Last glacial maximum paleochemistry and deepwater circulation in the Southern Ocean: Evidence from foraminiferal cadmium, *Paleoceanography*, *12*, 787–796.

Rosenthal, Y., M. P. Field, and R. M. Sherrell (1999), Precise determination of element/calcium ratios in calcareous samples using sector field inductively coupled plasma mass spectrometry, *Anal. Chem.*, *71*, 3248–3253.

Sarnthein, M., K. Winn, S. J. A. Jund, J.-C. Duplessy, L. Labeyrie, H. Erlenkeuser, and G. Ganssen (1994), Changes in east Atlantic deepwater circulation over the last 30,000 years: Eight time slice reconstructions, *Paleoceanography*, *9*, 209–268.

Schrag, D. P., J. F. Adkins, K. McIntyre, J. L. Alexander, D. A. Hodell, C. D. Charles, and J. F. McManus (2002), The oxygen isotopic composition of seawater during the Last Glacial Maximum, *Quat. Sci. Rev.*, *21*, 331–342.

Schulz, H., U. von Rad, and H. Erlenkeuser (1998), Correlation between Arabian Sea and Greenland climate oscillations of the past 110,000 years, *Nature*, *393*, 54–57.

Sigman, D. M., and E. A. Boyle (2000), Glacial/interglacial variations in atmospheric carbon dioxide, *Nature*, *407*, 859–869.

Sigman, D. M., S. J. Lehman, and D. W. Oppo (2003), Evaluating mechanisms of nutrient depletion and ^{13}C enrichment in the intermediate-depth Atlantic during the last ice age, *Paleoceanography*, *18*(3), 1072, doi:10.1029/2002PA000818.

Stephens, B. B., and R. F. Keeling (2000), The influence of Antarctic sea ice on glacial-interglacial CO_2 variations, *Nature*, *404*, 171–174.

Stocker, T. F., and D. G. Wright (1991), Rapid transitions of the ocean's deep circulation induced by changes in surface water fluxes, *Nature*, *351*, 729–732.

Stommel, H. (1958), The abyssal circulation, *Deep Sea Res.*, *5*, 80–82.

Stommel, H., and A. B. Arons (1960), On the abyssal circulation of the world ocean - I. Stationary planetary flow pattern on a sphere, *Deep Sea Res.*, *6*, 140–154.

Tachikawa, K., and H. Elderfield (2002), Microhabitat effects on Cd/Ca and $\delta^{13}C$ of benthic foraminifera, *Earth Planet. Sci. Lett.*, *202*, 607–624.

Toggweiler, J. R. (1999), Variation of atmospheric CO_2 by ventilation of the ocean's deepest water, *Paleoceanography*, *14*, 571–588.

Toggweiler, J. R., and B. Samuels (1995), Effect of Drake Passage on the global thermohaline circulation, *Deep Sea Res.*, *Part I*, *42*, 477–500.

Toggweiler, J. R., and B. Samuels (1998), On the ocean's large-scale circulation near the limit of no vertical mixing, *J. Phys. Oceanogr.*, *28*, 1832–1852.

Toggweiler, J. R., J. L. Russell, and S. R. Carson (2006), Midlatitude westerlies, atmospheric CO_2, and climate change during the ice ages, *Paleoceanography*, *21*, PA2005, doi:10.1029/2005PA001154.

Wang, Y. J., H. Cheng, R. L. Edwards, Z. S. An, J. Y. Wu, C.-C. Shen, and J. A. Dorale (2001), A high-resolution absolute-dated Late Pleistocene monsoon record from Hulu Cave, China, *Science*, *294*, 2345–2348.

Warren, B. (1990), Suppression of deep oxygen concentrations by Drake Passage, *Deep Sea Res.*, *Part A*, *37*, 1899–1907.

Weyl, P. K. (1968), The role of the oceans in climatic change: A theory of the ice ages, *Meteorol. Monogr.*, *8*, 37–62.

Willamowski, C., and R. Zahn (2000), Upper ocean circulation in the glacial North Atlantic from benthic foraminiferal isotope and trace element fingerprinting, *Paleoceanography*, *15*, 515–527.

Zahn, R., and A. Stüber (2002), Suborbital intermediate water variability inferred from paired benthic foraminiferal Cd/Ca and $\delta^{13}C$ in the tropical West Atlantic and linking with North Atlantic climates, *Earth Planet. Sci. Lett.*, *200*, 191–205.

Zahn, R., K. Winn, and M. Sarnthein (1986), Benthic foraminiferal $\delta^{13}C$ and accumulation rates of organic carbon: *Uvigerina peregrina* group and *Cibicidoides wuellerstorfi*, *Paleoceanography*, *1*, 27–42.